

Analysis for Behavior of RC Arches with Openings and Strengthened by CFRP Laminates

Prof. Dr. Ammar Y. Ali

Bashar Abid Hamza

Babylon University, Engineering College, Civil Department.

Abstract

The main objective of the research reported in this paper was to present an experimental and analytical study to investigate the behavior and performance of reinforced concrete arches with and without openings, unstrengthened and strengthened (externally by CFRP laminates or internally by steel reinforcement). To meet the objective, twelve reinforced concrete semi circular arches with and without web openings were tested with cross section of (150*250)mm and inner diameter 1500mm and outer diameter 2000mm. The experimental variables considered in the test program included: curvature forces, location of opening through profile of arch, presence of internal strengthening by reinforcing steel (stirrups) or external strengthening by CFRP laminates for openings. The experimental results showed a significant decrease in ultimate load capacity by about 38% of that for control arch, with splitting mode failure which were registered for arches without confining stirrups to resist curvature forces in radial direction. The use of CFRP laminates as external confinement at the middle sector to resist curvature forces induced between reinforcing bars and concrete cover, which gave approximately the same general response, but the ductility ratio was lesser. The increase in load capacity for hinge-roller arch containing an opening at zone of excessive compressive force (near the support) was 39% and 43% more than for zones of pure bending and combined bending, shear force and axial compressive force, respectively. The proposed design method used in the current study for externally strengthening of opening by CFRP laminates at zones of pure bending, combined bending, shear force and axial compressive force, and excessive compressive force (near the support) gave good results, where the enhancement of the ultimate load of strengthened arch about 100%, 87% and 58%, respectively, when compared with unstrengthening arches that has same properties of openings, and gave conservative results when compared with solid control arch, where the ultimate load reached about 83%, 75% and 91%, respectively. ANSYS computer program (version 11.0, 2007) was performed throughout this study. Full bond was assumed between the CFRP and concrete surface and between the steel reinforcement and concrete. Brick element SOLID65 and SOLID45 was used to represent concrete element and steel plate, respectively. While LINK8 and SHEEL41 were used to represent steel reinforcement and CFRP sheets respectively. In general, a good agreement between the finite element solutions and experimental results has been obtained concerning estimate load-deflection response, mode of failure. And cracking and ultimate loads with average difference about 5.83% and 3.92%, respectively.

الخلاصة

ان الهدف الاساس من هذا البحث هو تقديم دراسة عملية وتحليلية عن تصرف وأداء الاعتاب الخرسانية المسلحة المقوسة الحاوية على فتحات والغير حاوية على فتحات والمقواة والغير مقواة باستعمال (اللداين الكربونية المسلحة او قضبان حديد التسليح). من أجل القيام بالدراسة المشار اليها اعلاه تم اعداد وفحص اثنا عشر عتبا " خرسانيا" مقوسا" (نصف دائرة) وبأبعاد مقطع (150*250) ملم وبقطر داخلي (1500ملم) وقطر خارجي (2000) ملم. المتغيرات التي يتضمنها البرنامج العملي هي تأثير قوة التقوس وموقع الفتحة خلال المقطع الطولي للعتب المقوس (حيث يتم دراسة تأثير تغير القوى الداخلية خلال المقطع الطولي للعتب المقوس) وتقوية الاعتاب المقوسة الحاوية على فتحات باستعمال (اللداين الكربونية المسلحة او قضبان حديد التسليح). اظهرت النتائج المختبرية نقصان ملحوظ في قابلية التحمل القصوى حوالي 38% للعتب المقوس الغير مقوى بحديد تسليح للتحمل قوى الناتجة من التقوس. نمط الفشل للنموذج الغير مقوى ضد قوى التقوس هو فشل انشطاري (splitting failure) وهذا الفشل يحصل بشكل مفاجئ وبدون تحذيرات متقدمة. ان استخدام اللداين الكربونية المسلحة بدلا من قضبان حديد التسليح لمقاومة القوى الناتجة من التقوس اعطت تحمل اقصى مقارب مع نقصان المطيلية بالمقارنة مع نموذج السيطرة. وجد زيادة في التحمل الاقصى في حالة وجود الفتحة في منطقة بالقرب من المسند (عندما تكون قوى الانضغاط المحورية مؤثرة بشكل رئيسي) أعلى عن حالة وجود الفتحة في منطقتي (العزم الصرف و تراكب) عزم , قوى قص وقوى الانضغاط المحوري) بمقدار (39%, 43%) بالترتيب. طريقة التصميم المقترحة في الدراسة الحالية للتقوية للفتحة باستخدام اللداين الكربونية المسلحة في منطقة [العزم الصرف , تراكب) عزم , قوى قص وقوى الانضغاط المحوري) , بالقرب من المسند (عندما تكون قوى الانضغاط المحورية مؤثرة بشكل رئيسي)] تعطي نتائج جيدة, حيث أعطت زيادة في التحمل الاقصى للعتب المقوى بمقدار (100%, 87%, 58%) , بالترتيب, بالمقارنة مع نفس النموذج الغير مقوى. ايضا تحسن التحمل الاقصى حيث بلغ (83%, 75%, 91%) , بالترتيب, من التحمل الاقصى لعتب السيطرة. من جهة اخرى, العمل التحليلي قدم نموذجا لاختبار ثلاثي الأبعاد للعناصر المحددة ملائماً لتحليل الاعتاب الخرسانية المسلحة المقوسة الحاوية على فتحات والغير حاوية على فتحات والمقواة والغير مقواة باستعمال (اللداين الكربونية المسلحة او حديد التسليح) تحت تأثير أحمال ترايديه باستخدام برامج الحاسوب (ANSYS 11.0). وبشكل عام تم الحصول على توافق بين النتائج المستحصلة من طريقة العناصر المحددة والنتائج المختبرية المتوفرة للهطول ونمط الفشل وأحمال التشقق والاقصى وبمعدل فرق 5,83% و 3,92% بالترتيب.

Introduction

An arch may be defined as a curved girder having convexity upwards, and supported at its ends. The shape of the arch may be circular, elliptical or parabolic and sometimes it is made up by circular arcs of several and different radii or/and centers. It may be subjected to in plane: vertical, horizontal or even inclined loads. In the past, the arches had been the backbone of the important buildings. The main aim of arch is to enhance the load carrying capacity, which may come from the stiffening behavior due to membrane action. However, because of relatively smaller values of bending moments and tensile stresses induced in the arch rib in comparison with the straight beam, it is preferred to utilize arched girders in structural purposes. Also, this characteristic enabled structural engineers to achieve large spans in buildings roofing and bridges

decking using materials with efficient compressive strength, like concrete, or using suitable compression resisting systems, like braced and trussed metal structures to overcome the dominant compressive stresses generated in the arches. Arching not only reduces the bending moment in the arch in comparison with a straight member of same properties and loading patterns, but even more the shear force. On the other hand, an axial force is introduced due to the arch action. This state of action is compatible with concrete materials, which is relatively weak in carrying tension and shear stresses, but adequate in carrying compressive stresses. Hence, reinforced concrete material is efficient in the construction of some arched structures such as gable frames and arched bridges, beams of shell and domes(Hamza, 2013).

Opening in Reinforced Concrete Beams

In the construction modern buildings, a network of pipes and ducts is necessary to accommodated essential services like water supply, sewage, air-conditioning, electricity, telephone, and computer network. Usually, these pipes and ducts are placed underneath the beam soffit and, for aesthetic reasons, are covered by a suspended ceiling, thus creating a dead space. Passing these ducts through transverse opening in the floor beams leads to a reduction in the dead space and result in a more compact design. For small buildings, the saving thus achieved may not be significant, but for multistory buildings, any saving in story height multiplied by the number of stories can represent a substantial saving in total height, length of air-conditioning and electrical ducts, plumbing risers, walls and partition surfaces, and overall load on the foundation (Mansur, 2006). Figure 1, shows a view of the typical layout of pipes for building.

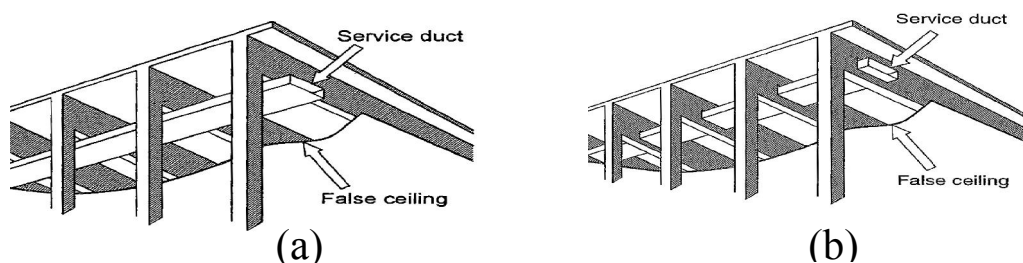


Figure 1: Typical Layout of Pipes for High Rise Building (Mansur and Hasnat, 1979).

a- Typical layout of service ducts.

b- Alternative arrangement of service ducts

It is obvious that inclusion of openings in beams alters the simple beam behavior to a more complex one. Due to abrupt changes in sectional configuration, opening corners are subject to high stress concentration that may lead to cracking unacceptable from aesthetic and durability viewpoints. The reduced stiffness of the beam may also give rise to excessive deflection under service load and result in a considerable redistribution of internal forces and moments in a

continuous beam. Unless special reinforcement is provided in sufficient quantity with proper detailing, the strength and serviceability of such a beam may be seriously affected(Mansur, 2006).

In practice, the most common shapes of openings are circular and rectangular. Circular openings are required to accommodate service pipes, such as for plumbing, while rectangular openings provide the passage for air-conditioning ducts that are generally rectangular in shape.

With regard to the size of openings, many researchers use the terms “small” and “large” without any definition or clear-cut demarcation line. Mansur and Hasnat(1979) have defined small openings as those circular, square or nearly square in shape. Whereas, according to Sones and Corley(1974), a circular opening may be considered as effected when its diameter exceeds 0.25 times the depth of the web because introduction of such openings reduces the strength of the beam. The authors however considers that the essence of classifying an opening either small or large lie in the structural response of the beam. When the opening is small enough to maintain the beam-type behavior or, in other words, if the usual beam theory applies, then the opening may be termed as small opening. In contrast, large openings are those that prevent beam-type behavior to develop(Mansur, 2006;Mansur, 1998).

For small openings, two different failure modes are identified. These types of failure may be labeled as "beam-type" failure and "frame-type" failure, respectively, and required separate treatment for complete design. In contrast, for large openings the beam-type behavior transforms into a Vierendeel action(Figure 2) as the size of opening is increased. Since the behavior of a beam depend on the size of opening, small and large openings need separate treatment in design (Mansur, 1998).

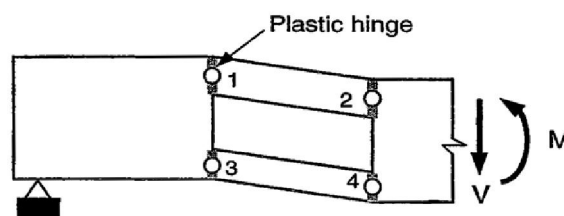


Figure 2:Collapses Mechanism at Large Opening(Mansur and Hasnat,1979)

The effects introducing an opening on the overall response of a beam may be summarized as follow (Mansur and Hasnat,1979):

- 1- Introduction of an opening in the web of a beam leads to early diagonal crack, and the load at first crack decreases with an increase in either the length or the depth of opening.

- 2- Unless additional reinforcement is provided to restrict the growth of cracks, the opening corners are liable to exhibit wide cracking.
- 3- When that the same amount and scheme of reinforcement is used, an increase in the opening size either by increasing the length or the depth of opening decreases the strength as well as stiffness of the beam. The eccentricity of opening, however, has only a marginal effect on both strength and stiffness.
- 4- The chord members above and below the opening behaves in a manner similar to the chords of a Vierendeel panel with contraflexure points located approximately at mid-span of the chords. Final failure occurs by the formation of a mechanism with four hinges in the chords, one at each corner of the opening as shown in Figure 2.

Experimental Work

The experimental program includes twelve simply supported RC semi circular arches with and without web openings . All arches were of inner diameter 1500mm and outer diameter 2000mm, and had cross section dimensions 250mm overall depth and 150mm width. All arches were tested under two point loads at extrados (top) surface. Figure 3 shows the geometrical details of arches and the steel reinforcement provided with a clear concrete cover to the reinforcement of 25mm. Two Ø12 mm deformed bars were provided as tension reinforcement and two Ø10 mm top deformed bars to fastened the stirrups. All arches were provided with closed stirrups of Ø6 mm spaced at 6.25° along the circular path (95mm along arch center line), The stirrups were placed at middle-third of span to resist curvature forces, except arches B1, B11 and B12 which are without stirrups at middle-third (middle-sector) of span length.

The arches were divided into four groups: the first group was without opening and the other three included opening of dimensions (100*200 mm) at midspan(90°), at angle 45° and 15° , respectively. Table 1 illustrates the description for each tested arch.

Arches without Opening

This group consists of four arches. Two arches without stirrups at middle –third(middle-sector) of beam span (B1 and B11). The third arch is with CFRP straps instead of closed stirrups at middle –third (middle-sector) of the span(B12). The last arch is with stirrups at middle-third of the span as control arch(B2).

Arches with Opening

Arches with openings consists of three groups. The first group consists of three arches with opening at midspan. The second group consists of three arches with openings at 45° . The third group consists of two arches with openings at 15° . For each group, the first arch of opening without

strengthening, the second arch of opening were strengthened by CFRP straps and the last arch of opening strengthened by internal steel reinforcement. Table 1 and Figure 3 illustrates the details for each tested arch.

Table 1: Description of Tested Arches

Group No.	*Arch Designation	**Location of Openings	Details			
			Web Reinforcement(Stirrups)		External CFRP Laminates	
			At Middle Sector	Around the Openings	At Middle Sector	Around the Openings
1st Group without openings	B1(Pilot)	--	--	--	--	--
	B2		Ø6@6.25°		--	
2nd Group with openings at $\Theta=90^\circ$ (midspan)	B3(90°)	Midspan $\Theta=90^\circ$	Ø6@6.25°	--	--	--
	B4(90°-CF)			--	--	CFRP straps (2 of 40mm width on each side and 3 of 25mm width for each chord)
	B8(90°-S)			3Ø6 stirrups for each chord and 2Ø10 diagonal bars for each corner	--	--
3rd Group with openings at $\Theta=45^\circ$ (quarter)	B5(45°)	$\Theta=45^\circ$	Ø6@6.25°	--	--	--
	B6(45°-CF)			--	--	CFRP straps (1 of 75mm width on each side and 3 of 25mm width for each chord)
	B10(45°-S)			stirrups (6Ø6 for each chord and 2Ø6 full depth on each side)and 2Ø10 diagonal bars for each corner	--	--
4th Group with openings at $\Theta=15^\circ$ (near support)	B7(15°)	$\Theta=15^\circ$	Ø6@6.25°	--	--	--
	B9(15°-CF)			--	--	CFRP straps (1 of 75mm width on each side and 3 of 25mm width for each chord)
Group without openings	B11	--	--	--	--	--
	B12				8 CFRP straps of 30mm width	

* The number inside bracket refer to position of opening.

S:refers to strengthening of opening by internal stirrups.

CF: refers to strengthening of opening by external CFRP laminates.

** Θ :measured from support.

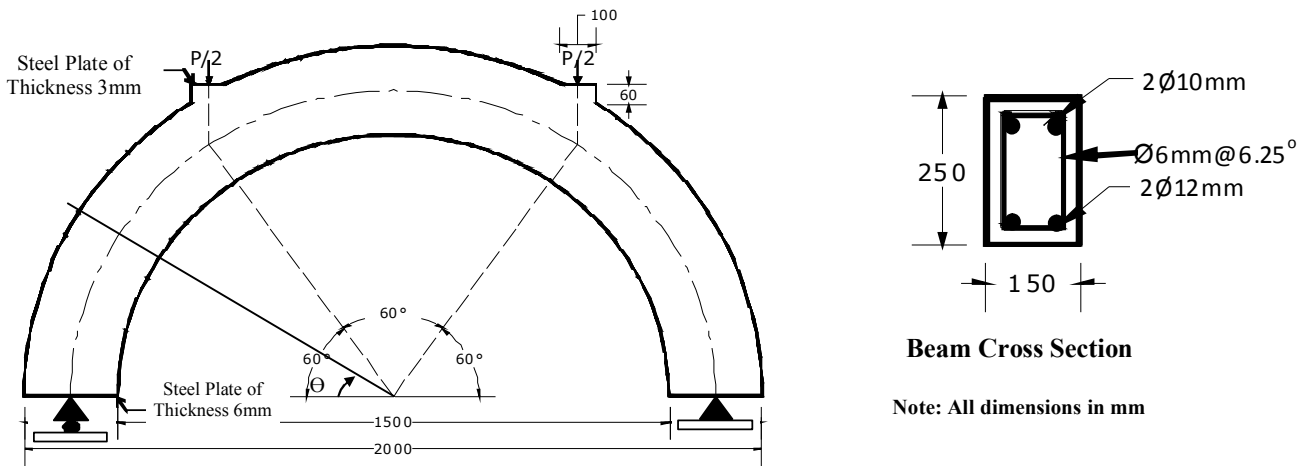


Figure 3: Geometry and Reinforcement Details of the Tested Arches

Strengthening System

Strengthening system is chosen carefully according to crack pattern. The method of design adopted for strengthening technique had been suggested by (Mansur, 1998) for straight beam. The design specification of ACI 318-2011 and ACI Committee 440-2002 was satisfied for steel bars reinforcement and CFRP laminates, respectively.

External Strengthening by CFRP Straps

Arch B12 was strengthened by eight full wrap of CFRP straps of 0.131mm thickness and 30 mm width at middle-third of beam span as shown in Figure 4. Arch B4(90-CF) were strengthened by full wrap of CFRP straps of 0.131mm thickness with pair of 40mm width on each side of the opening and three pairs of 25mm width for both top and bottom chords of opening, as shown in Figure 5. Arches B6(45-CF) and B9(15-CF) were strengthened by full wrap of CFRP straps of 0.131mm thickness with 75mm width on each side of the opening and three pairs of 25mm width for both top and bottom chords of opening, as shown in Figures 6 and 7, respectively.

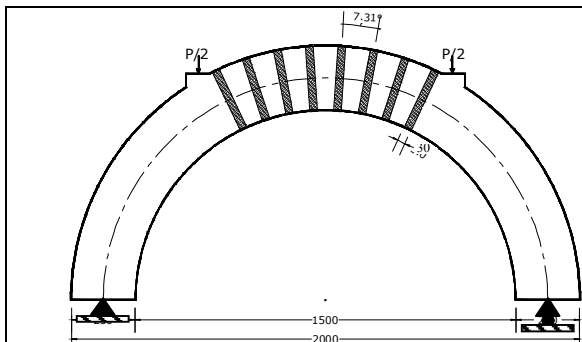


Figure 4-a: External Strengthening with CFRP of Arch B12

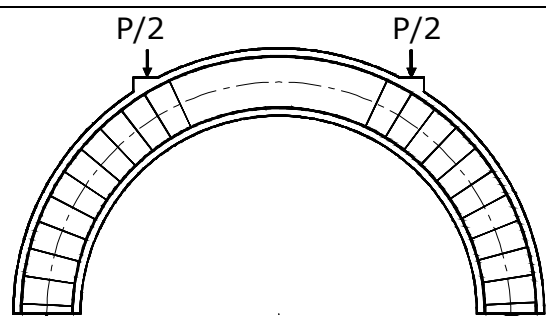


Figure 4-b: Internal Reinforcements of Arch B12

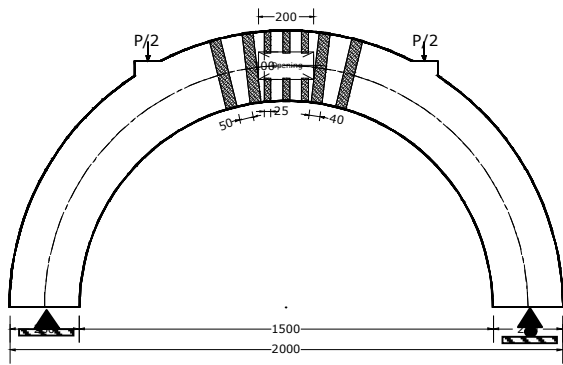


Figure 5-a: External Strengthening with CFRP of Arch B4(90-CF)

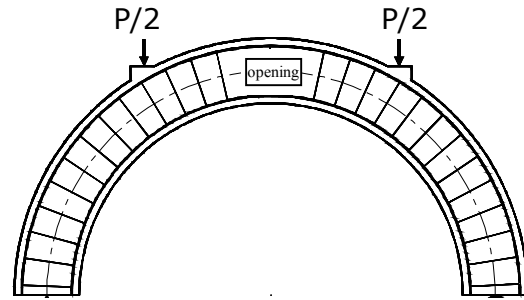


Figure 5-b: Internal Reinforcements of Arch B4(90-CF)

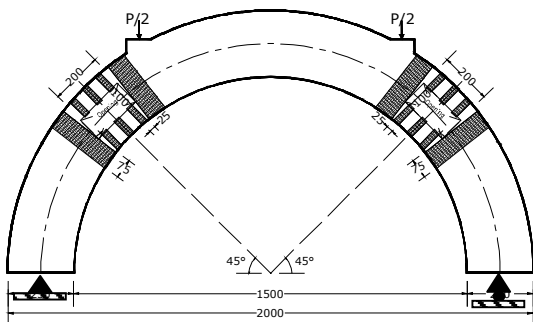


Figure 6-a: External Strengthening with CFRP of Arch B6(45-CF)

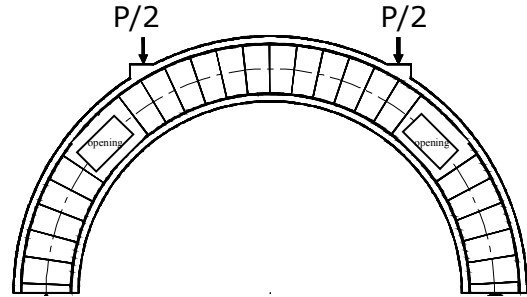


Figure 6-b: Internal Reinforcements of Arch B6(45-CF)

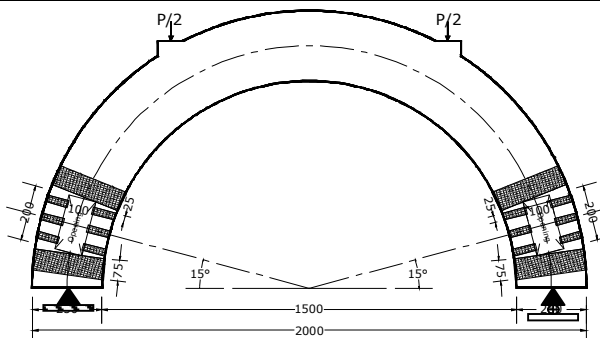


Figure 7-a: External Strengthening with CFRP of Arch B9(15-CF)

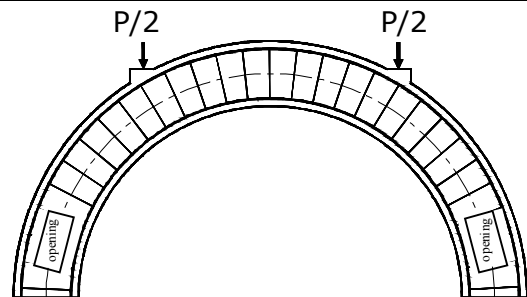


Figure 7-b: Internal Reinforcements of Arch B9(15-CF)

Internal Strengthening by Internal Reinforcement

Arch B8(90-S) were strengthened by three pairs of closed stirrups of $\varnothing 6$ mm for both top and bottom chords of opening and two diagonal bars $\varnothing 10$ mm for each corner of opening as shown in Figure 8. Arch B10(45-S) were strengthened by two full depth closed stirrups $\varnothing 6$ mm on each side of the opening, six pairs deformed bars of $\varnothing 6$ mm closed stirrups for both top and bottom chords of opening and two diagonal bars $\varnothing 10$ mm for each corner of opening as shown in Figure 9. A typical cross section through opening of arches B8(90-S) and B10(45-S) is shown in Figure 10.

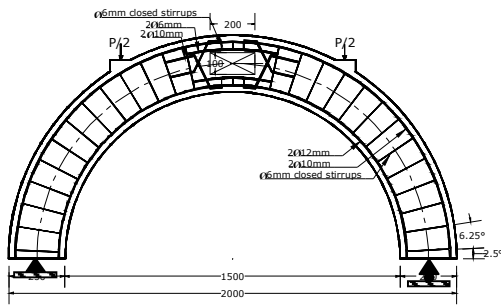


Figure 8: Internal Strengthening of Arch B8(90-S)

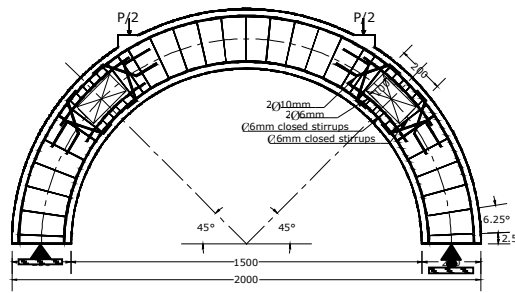


Figure 9: Internal Strengthening of Arch B10(45-S)

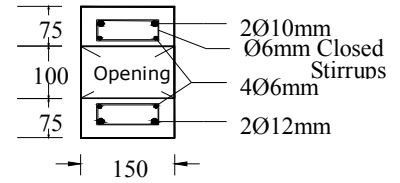


Figure10:Internal Strengthening of Arches B8(90-S) and B10(45-S) (Section Through Opening)

Material Properties

Normal weight concrete was used to cast arches. The concrete compressive strength at time of testing (more than 28 days) are listed in Table 2. The deformed bars have (520,470 and 525) MPa yield stress for bar diameters (6, 10 and 12)mm, respectively. A CFRP sheet has a tensile strength of 4300 MPa, and modulus of elasticity of 238000 MPa, the elongation at break of 1.8% and the thickness of 0.131mm (Sika,2005).

Table 2: Concrete Compressive Strength of Arches

Arch No.	B1	B2	B3(90)	B4(90-CF)	B5(45)	B6(45-CF)	B7(15)	B8(90-S)	B9(15-CF)	B10(45-S)	B11	B12
Compressive strength of concrete (f'_c) (MPa)	32.8	36.5	33.3	38.34	32.0	34.2	32.4	34.1	35.61	37.4	36.1	33.0

3.7 Instrument and Test Procedure

All of the arch beams were tested under two third point loading, with the load applied at angle 60° from each support as shown in Figure 11. Arches were tested as simply supported (hinge-roller) in 1500 kN hydraulic testing machine as shown in Figure 12. The main characteristics of the structural behavior of the arch specimens were detected at every stage of loading during testing. A dial gage of 0.01 mm accuracy was used at the midspan of the arch and at the roller support in order to calculate the deflection and horizontal displacement of roller support, respectively. The specimens were placed on the supports of the testing machine, and then the first readings of the gages were recorded. After that, the specimens were loaded with a constant rate of loading. Readings of deflection and horizontal displacement of roller support were recorded at each interval of load as well as recording the first crack load, tracing the cracking patterns and the failure load consequently.

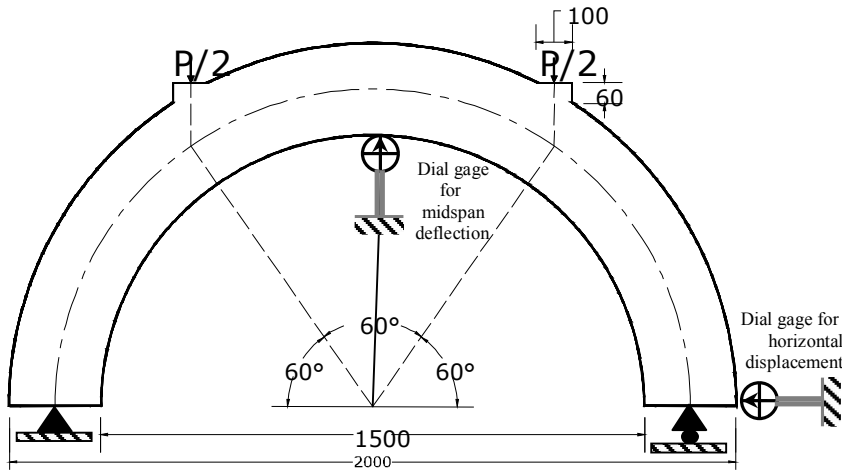


Figure 11: Loading Details of Test Arch Specimens



Figure 12: Loading Machine Used in the Test

Experimental Results

The main objective of the current research work is to investigate the behavior of reinforced concrete arches with openings and strengthened by CFRP laminates . Table 3 shows a summary for the test results. Test results were discussed based on load-midspan deflection and load–horizontal displacement of roller support to explore the influence of internal strengthening with both stirrups and diagonal bars and external strengthening with CFRP laminates on cracking and ultimate loads, crack pattern, post-cracking stiffness, ductility ratio and failure modes.

Table 3: Summary of Tested Arches

Arch		Cracking load, kN P_{cr}	Ultimate load, kN P_u	Percentage of Ultimate Load with Respect to Arch B2	Ductility Ratio	Failure Mode
Arches without Opening	Pilot(B1)	43.1	86.2	54	--	Splitting failure
	Unconfined B11	43.1	99.1	62	1.38	Splitting failure
	Internally Confined B2	38.8	159.5	--	5.9	Flexural failure
	Externally Confined B12	60.3	163.8	102.7	3.72	Rupture of CFRP
Arches with Opening at Midspan	Unstrengthened B3(90)	32.3	66.8	42	<1.0	Compression failure of top chord
	Internally Strengthened B8(90-S)	25.8	142.2	89	6.34	Flexural failure
	Externally Strengthened B4(90-CF)	34.5	133.6	83	6.72	Rupture of CFRP
Arches with Openings at angle 45°	Unstrengthened B5(45)	25.8	64.6	40	<1.0	Shear failure
	Internally Strengthened B10(45-S)	43.1	129.3	81	2.04	Shear failure
	Externally Strengthened B6(45-CF)	38.8	120.7	75	2.68	Shear failure
Arches with Openings at angle 15°	Unstrengthened B7(15)	32.3	92.7	58	1.75	Excessive compressive failure
	Externally Strengthened B9(15-CF)	34.5	146.5	91.8	5.1	Flexural failure

Arches without Opening

Unconfined B11 arch was performed without opening and without confining stirrups at middle sector to resist curvature forces. At early stages of loading, the arch deformation was initially within elastic ranges, then the applied load was increased until the first crack occurred which was observed at the maximum moment region between the two point loads at load level 43.1 kN. As the load was increased further, flexural – shear crack initiated in the tension face at load 56 kN as shown in Figure 13. As the load was increased further, circumference crack (along the longitudinal axis of tension reinforcement), also several flexural cracks initiated in the tension face at intervals along the span and propagated upward was observed at 59.7 kN. As the load was increased further, no one of the conventional failure modes was appeared. The failure mode occurred through suddenly splitting of concrete cover along tension reinforcement followed by circumference crack between two point loads. The reading of the failure load was 99.1 kN. Figure 13 shows mode of failure and cracks pattern, while Figure 14 show load – midspan deflection curve and load – horizontal displacement of roller support curve.

Arch B2 is a control specimen. The arch was loaded gradually until the first crack was observed. The first flexural cracks appeared in the constant moment region (middle sector) at a load of approximately 38.8 kN. Further flexural cracks formed and widened as the loading increased. As the load was increased further, flexural – shear crack initiated in the tension face at load of 56 kN as shown in Figure 13. The flexural cracks in the constant moment region widened with increasing load. Also, circumference crack (along the longitudinal axis of tension reinforcement) was observed at load of 73.3 kN . The presence of confining stirrups at the constant moment segment (middle sector) prevent splitting failure. Finally, the failure mode for arch B2 can be classified as flexural failure by yielding of steel in tension followed crushing of concrete at the compression fiber at load of 159.5 kN, as shown in Figure 13. The load – midspan deflection curve and load – horizontal roller support displacement curve are shown in Figure 14.

In externally confined B12 arch, the first flexural cracks appeared in the constant moment region (middle sector) at a load of approximately 60.3 kN. Further flexural cracks formed and widened as the loading increased. As the load was increased further, flexural – shear crack initiated in the tension face at load of 77.6 kN as shown in Figure 13. The flexural cracks in the constant moment region widened(has a width less than arch B2 at the same load stages) with increasing load. Also, circumference crack (along the longitudinal axis of tension reinforcement) was observed at load of 112 kN outside middle sector of arch span and at 155 kN between the two point loads. The presence of confining CFRP laminates at the constant moment

region (middle sector) prevent splitting failure at early stage. Finally, The failure mode occurred through suddenly rupture of CFRP laminates followed by circumference crack between two point loads at load of 163.8 kN, as shown in Figure 13. The load – midspan deflection curve and load – horizontal roller support displacement curve are shown in Figure 14.

It can be seen that the number of cracks of arch B12 has been reduced significantly due to the presence of CFPR laminates along the middle sector of the span. Also, up to first crack load, the presence of CFPR laminates along the middle sector of the arch span (arch B12) was not effect the deflection (midspan and horizontal displacement of roller support) significantly. As the load increased further after cracking, the presence of CFRP laminates increase arch stiffness (reduce deflection) significantly and reduce ductility ratio(ratio of deflection at ultimate load to the deflection at yielding(Ali 2006)) for arch B12 by about 37% when compared with arch B2, whereas the increase in ultimate load by about 2.7%.

It can be concluded that when provide stirrups in arch B2 or CFRP laminates in arch B12 at constant moment region, increase the load capacity for arches B2 and B12 by about (61% and 65%), respectively when compared with that arch B11, Table 3. The reducing in the load capacity of arch B11 caused from forces in radial direction. These forces act on the concrete cover in a manner similar to beam on elastic foundation which led to splitting concrete cover. The formations of the radial forces are as a result of the axial force in the main tensile steel reinforcing bars.

Arches with opening at midspan(Pure bending moment region)

The arch B3(90) include opening at midspan and without strengthening. The arch deformation was initially within the elastic ranges at the early stages of loading. Then, the load was increased until the first crack occurred which was observed in the maximum moment region between the two point loads. The cracking load occurred at 32.3 kN. The diagonal crack starts from bottom corner of opening at left side at load of 43.1kN. As the load was increased further, several flexural cracks initiated in the tension face at intervals along the span and moved upwards, also, diagonal crack starts from other corners of opening. As the load was increased further, flexural-shear cracks initiated at load of 51.7 kN , Figure 13. As the load was increased further, no one of the conventional failure modes was appeared. Arch B3(90) failed at a load of 66.8 kN by forming two diagonal cracks start from the top corners of opening, then the cracks growth along top reinforcement toward the two point loads until failure occurs, Figure 13. The

load–midspan deflection curve and load–horizontal displacement of roller support curve shown Figure 14.

Internally Strengthened B8(90-S)arch include opening at midspan and strengthened by three pairs closed stirrups of Ø6 mm for both top and bottom chords of opening and two diagonal bars Ø10 mm for each corner of opening. The arch deformation was initially within the elastic ranges at the early stages of loading, the load was increased until the first crack occurred which was observed in the maximum moment region between the two point loads. The cracking load occurred at 25.8 kN. The diagonal crack starts from bottom corner of opening at left side at load of 30.2 kN. As the load was increased further, several flexural cracks initiated in the tension face at intervals along the span and moved upwards, also, diagonal crack starts from other corners of opening. As the load was increased further, flexural – shear crack initiated in the tension face at load of 90.5 kN as shown in Figure 13. In spite of forming diagonal corner cracks for arch B8(90-S), the arch fail due to crushing of concrete at the compression fiber at load of 142.2 kN, Figure 13. The load – midspan deflection curve and load – horizontal displacement of roller support curve shown in Figure 14.

Externally Strengthened B4(90-CF) arch, include opening at midspan and strengthened by full wrap of CFRP laminates of 0.131mm thickness (pair of 40mm width on the each side of the opening and three pairs of 25mm width for both top and bottom chords of opening). The arch deformation was initially within the elastic range at the early stages of loading, the load was increased until the first crack occurred which was observed in the maximum moment region between the two point loads. The cracking load occurred at 34.5 kN. As the load was increased further, several flexural cracks initiated in the tension face at intervals along the span and moved upwards. As the load was increased further, flexural – shear crack initiated in the tension face at left load of 51.7 kN. The diagonal crack starts from bottom corner of opening at left side at load of 77.6 kN. As the load was increased, diagonal crack starts from other corners of opening. Finally, The failure mode occurred through suddenly rupture of CFRP laminates at load of 133.6 kN, as shown in Figure 13. The load – midspan deflection curve and load – horizontal roller support displacement curve shown in Figure 14.

Table 3 shows that the percentage of the ultimate load for unstrengthened opening of arch B3(90) was 42% when compared with control arch B2, while the percentage of the ultimate load for internally strengthened opening of arch B8(90-S) and externally strengthened opening of arch B4(90-CF) were 89% and 83%, respectively, when compared with control arch B2. It can be seen that the increase in ultimate capacity for arch B4(90-CF) less than arch B8(90-S), this due to the

far distance between the CFRP strips and , hence, the diagonal crack does not reach the second CFRP strip, Figure 13. It can be conclude, that the method of design for straight beam with opening suggested by Mansur (1998), give a good result for RC arches at zone of pure bending moment. For the strengthened arches B8(90-S) and B4(90-CF), the ductility ratio increased by 7% and 14%, respectively, in comparison with control arch B2.

Arches with Openings at Angle 45°(Combined of moment , shear and axial force)

Unstrengthened B5(45) arch include opening at angle 45° and without strengthening. The arch deformation was initially within the elastic ranges at the early stages of loading, the load was increased until the first crack occurred which was observed in bottom chord of left opening. The cracking load occurred at 25.8 kN. The diagonal crack starts simultaneously, from bottom corner of opening at left side and the opposite top corner of opening at load of 30.2 kN. These diagonal cracks propagate and widen rapidly. As the load was increased, first flexural crack was observed at constant moment region at load of 38.8 kN. As the load was increased further, several flexural cracks initiated in the tension face at intervals along the span and moved upwards, Figure 13. As the load was increased further, no one of the conventional failure modes was appeared. Arch B5(45) failed at a load of 64.6 kN by forming two diagonal cracks start from the two opposite corners of opening, then the cracks growth rapidly until failure occurs (beam-type failure), Figure 13. The load–midspan deflection curve and load–horizontal displacement of roller support curve shown in Figure 14.

Internally Strengthened B10(45-S) arch include opening at angle 45° and strengthened by two full depth closed stirrups Ø6 mm on each side of the opening, six pairs deformed bars of Ø6 mm closed stirrups for both top and bottom chords of opening and two diagonal bars Ø10 mm for each corner of opening. The arch deformation was initially within the elastic ranges at the early stages of loading, the load was increased until the first crack occurred which was observed simultaneously, in the maximum moment region between the two point loads and in the bottom chord of the left opening. The cracking load occurred at 43.1 kN. The diagonal crack starts simultaneously, from bottom corner of opening at left side and the opposite top corner of opening at load of 51.7 kN. These diagonal cracks propagate and widen rapidly. As the load was increased further, several flexural cracks initiated in the tension face at intervals along the span and moved upwards, Figure 13. Arch B10(45-S) failed by formation of two independent diagonal cracks, one in each member bridging the two solid beam segments (frame – type failure) at load of 129.3 kN,

Figure 13. The load – midspan deflection curve and load – horizontal displacement of roller support curve shown in Figure 14.

Externally Strengthened B6(45-CF) arch include openings at angle 45° and strengthened by full wrap of CFRP strips of 0.131mm thickness (75mm width on the each side of the opening and three pairs of 25mm width for both top and bottom chords of opening). The arch deformation was initially within the elastic range at the early stages of loading, the load was increased until the first crack occurred which was observed in the maximum moment region between the two point loads. The cracking load occurred at 38.8 kN. As the load was increased further, several flexural cracks initiated in the tension face at intervals along the span and moved upwards, also, diagonal crack starts from corners of opening as shown in Figure 13. Finally, the arch B6(45-CF) failed by forming diagonal crack of the opposite corners lead to rupture of CFRP strips. The arch failed at a load of 120.7 kN, Figure 13. The load – midspan deflection curve and load – horizontal displacement of roller support curve shown in Figure 14.

Table 3 shows that the percentage of the ultimate load for unstrengthened opening of arch B5(45) was 40% when compared with control arch B2, while the percentage of the ultimate load for internally strengthened opening of arch B10(45-S) and externally strengthened opening of arch B6(45-CF) were 81% and 75%, respectively, when compared with control arch B2. It can be conclude, that the method of design for straight beam with opening suggested by Mansur (1998), give a reasonable result for RC arches at zone of combined moment, shear and axial force. For the strengthened arches B10(45-S) and B6(45-CF), the ductility ratio decreased by 66% and 55%, respectively, in comparison with control arch B2.

Arches with Openings at angle 15° (Excessive axial compressive force)

Unstrengthened B7(15) arch include openings at angle 15° and without strengthening. The arch deformation was initially within the elastic ranges at the early stages of loading, the load was increased until the first crack occurred which was observed in the maximum moment region between the two point loads. The cracking load occurred at 32.3 kN. As the load was increased further, several flexural cracks initiated in the tension face at intervals along the span and moved upwards. As the load was increased further, flexural-shear cracks initiated at load of 56 kN , Figure 13. Two cracks start from the two opposite corners of opening (top and bottom corners) at load of 77.6kN. The crack of top corner was a diagonal crack. While the crack of bottom corner propagate parallel to support reaction, Figure 13. As the load was increased further, no one of the conventional failure modes was appeared. Arch B7(15) failed at a load of 92.7 kN by

propagate and widen the two cracks of opposite corners as describe above. The load – midspan deflection curve and load – horizontal displacement of roller support curve shown in Figure 14.

Externally Strengthened B9(15-CF) arch include openings at angle 15° and strengthened by full wrap of CFRP strips of 0.131mm thickness (75mm width on the each side of the opening and three pairs of 25mm width for both top and bottom chords of opening). The arch deformation was initially within the elastic range at the early stages of loading, the load was increased until the first crack occurred which was observed in the maximum moment region between the two point loads. The cracking load occurred at 34.5 kN. As the load was increased further, several flexural cracks initiated in the tension face at intervals along the span and moved upwards. As the load was increased further, flexural – shear crack initiated in the tension face at load of 69 kN as shown in Figure 13. Finally, the failure mode for arch B9(15-CF) can be classified as flexural failure in tension by yielding of steel followed crushing of concrete at the compression fiber at load of 146.5 kN, Figure 13. Also, it can be seen that the opening disappeared any cracks. The load – midspan deflection curve and load – horizontal roller support displacement curve shown in Figure 14.

Table 3 shows that the percentage of the ultimate load for unstrengthened opening of arch B7(15) was 58%, while the percentage of the ultimate load for externally strengthened opening of arch B9(15-CF) were 91.8%, when compared with control arch B2. It can be conclude, that the method of design for straight beam with opening suggested by Mansur (1998), give a reasonable result for RC arches at zone of excessive axial force. For the strengthened arch B9(15-CF), the ductility ratio decreased by 13%, in comparison with control arch B2.

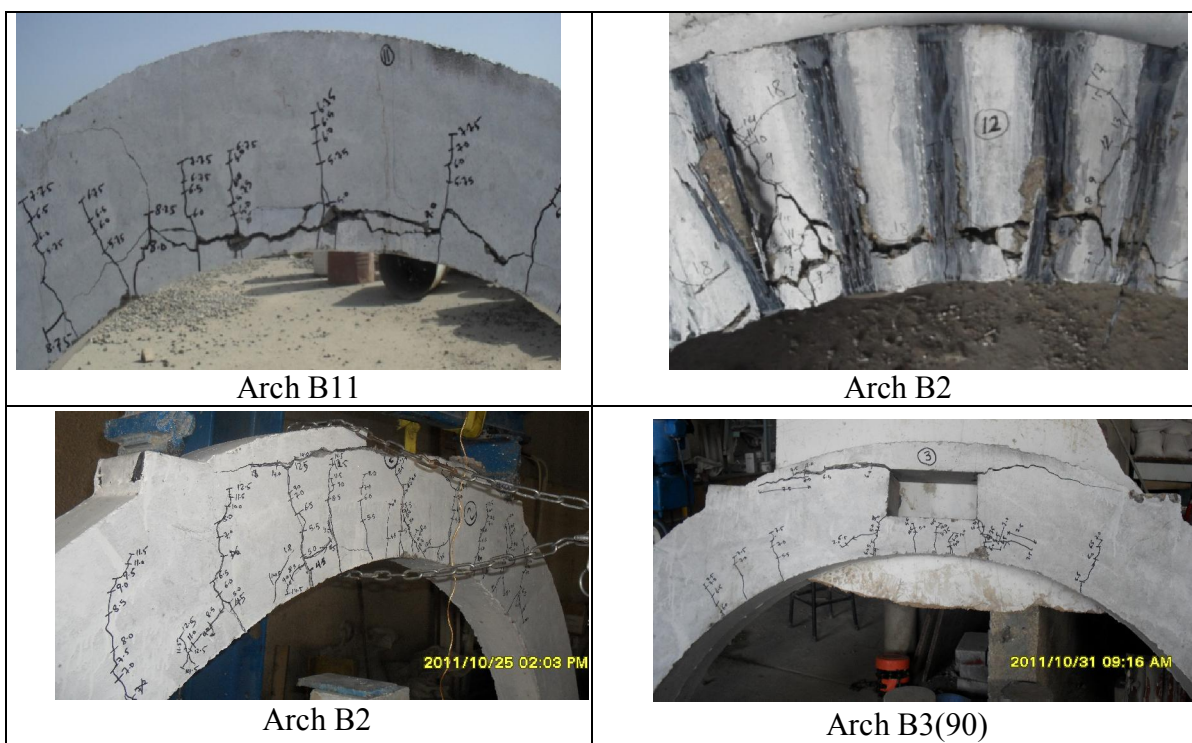




Figure 13: Modes of Failure

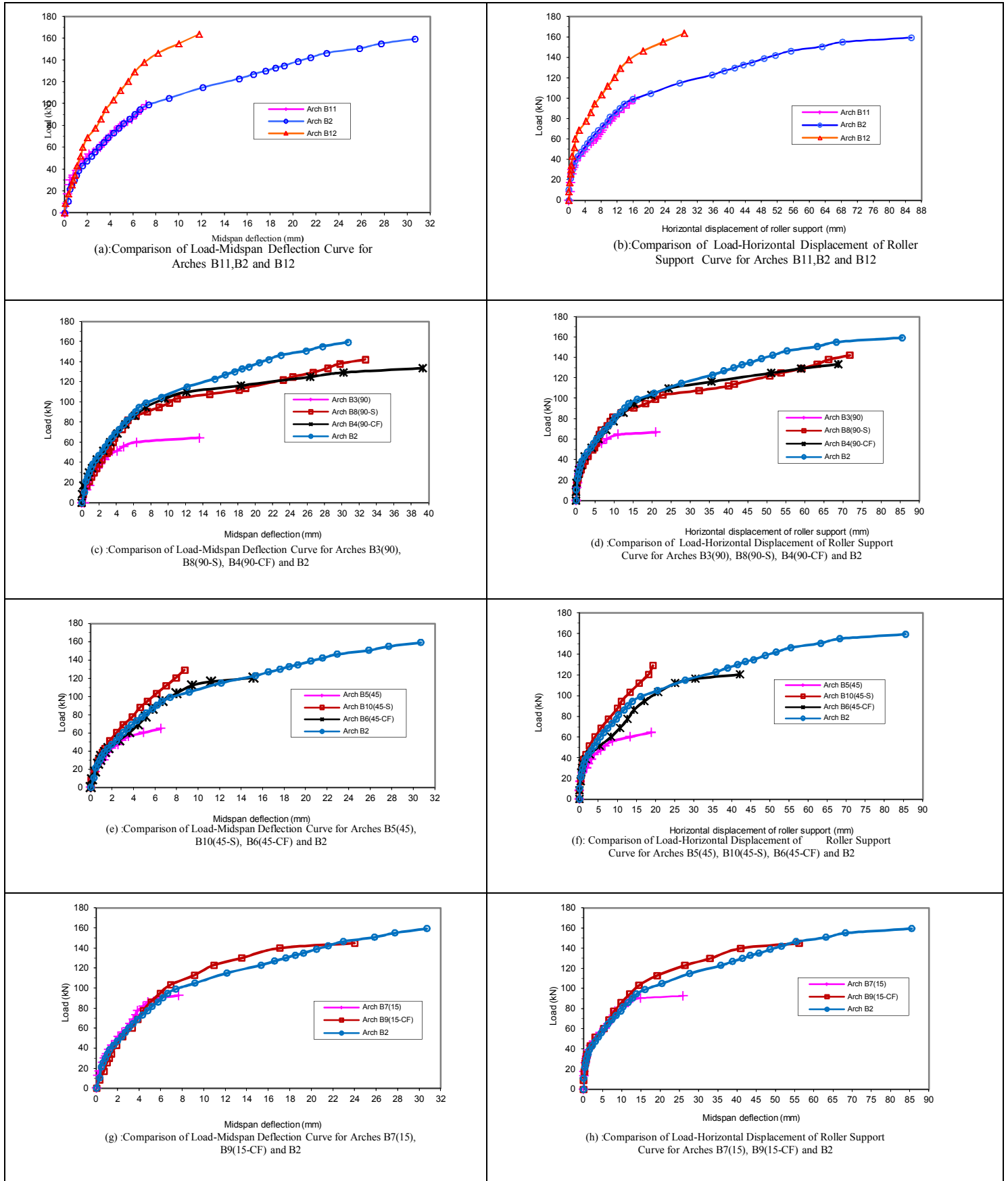


Figure 14 : Load-deflection curves for tested arches

Analytical Study

The analytical work included a three-dimensional nonlinear finite element model suitable for the analysis of reinforced concrete arches with or without openings and unstrengthened or strengthened by (CFRP laminates or reinforcing steel) under monotonic loading using the computer program ANSYS (Version 11.0, 2007). Full bond was assumed between the CFRP and concrete surface and between the steel reinforcement and concrete. Brick element SOLID65 and SOLID45 was used to represent concrete element and loading steel plates, respectively. While LINK8 and SHEEL41 were used to represent steel reinforcement and CFRP sheets respectively. Geometry of these elements was illustrated in Figure 15. The full Newton-Raphson Method was used for the nonlinear solution algorithm. The materials nonlinearity due to cracking, crushing of concrete, and yielding of reinforcement were taken into consideration during the analysis.

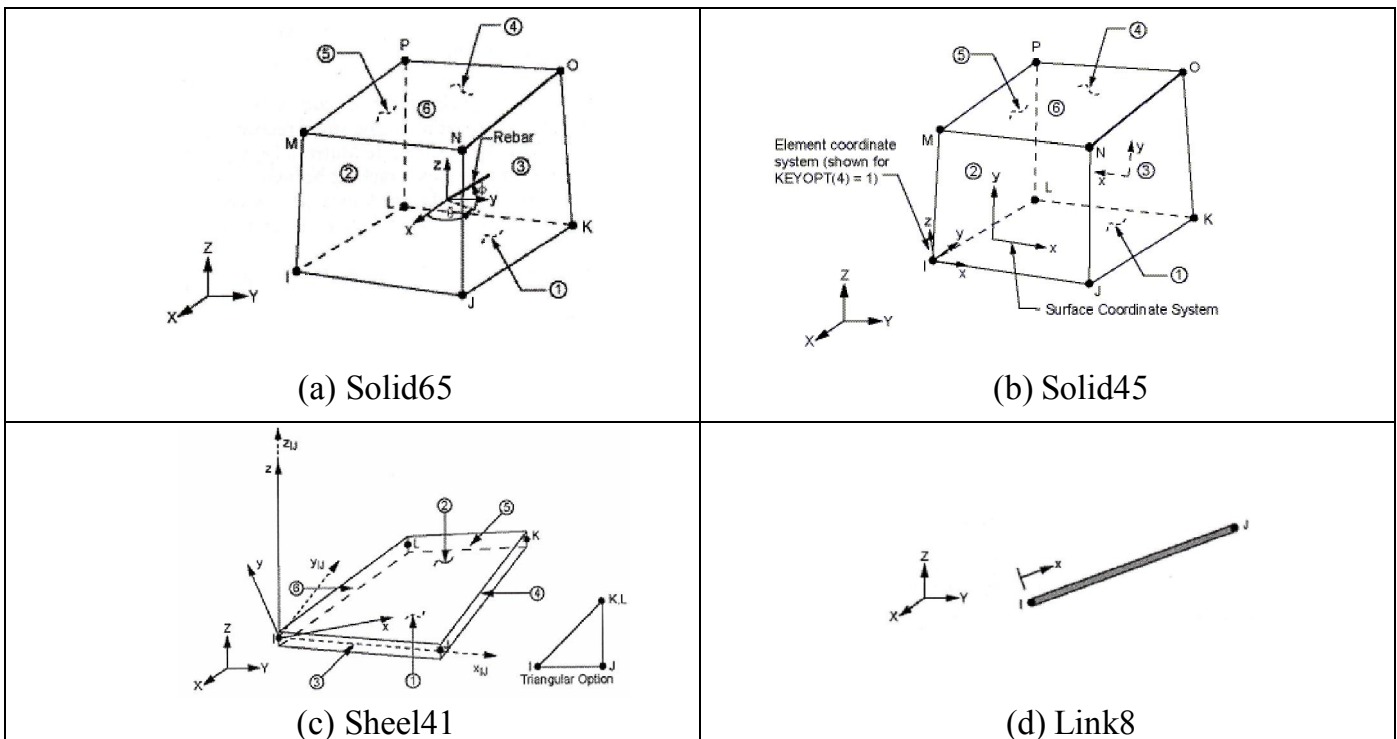


Figure 15: Geometry of Elements

Finite Element Mesh (Modeling)

Strains are the x and/or y derivatives of the displacements and thus depend on the distribution of the displacements for any given mesh. The strains and stresses may change in erratic way as the mesh is refined. When an increase in mesh has negligible on the results of the midspan deflection, it is assumed that the convergence of result is obtained. This convergence is found when the number of elements equals to 1392 elements for beam without opening (i.e 6, 4

and 58 elements in r , z and Θ -directions) and 1984 elements for beam with opening (i.e 8, 4 and 62 elements in r , z and Θ -directions) as shown in Figure 16.

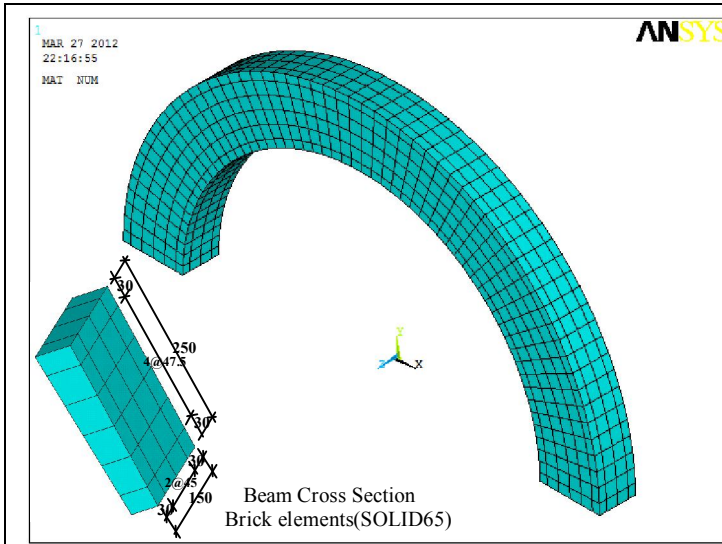


Figure 16-a: Mesh Modeling of Tested Concrete Arches without Opening

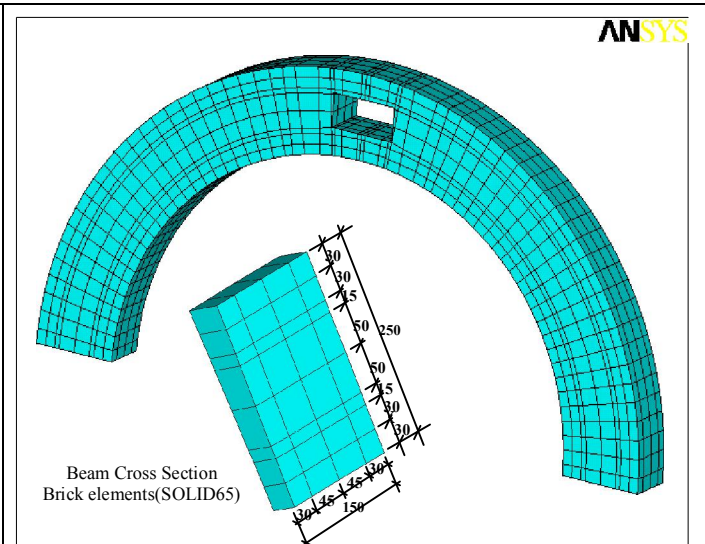


Figure 16-b: Mesh Modeling of Tested Concrete Arches with Opening

Finite Element Results

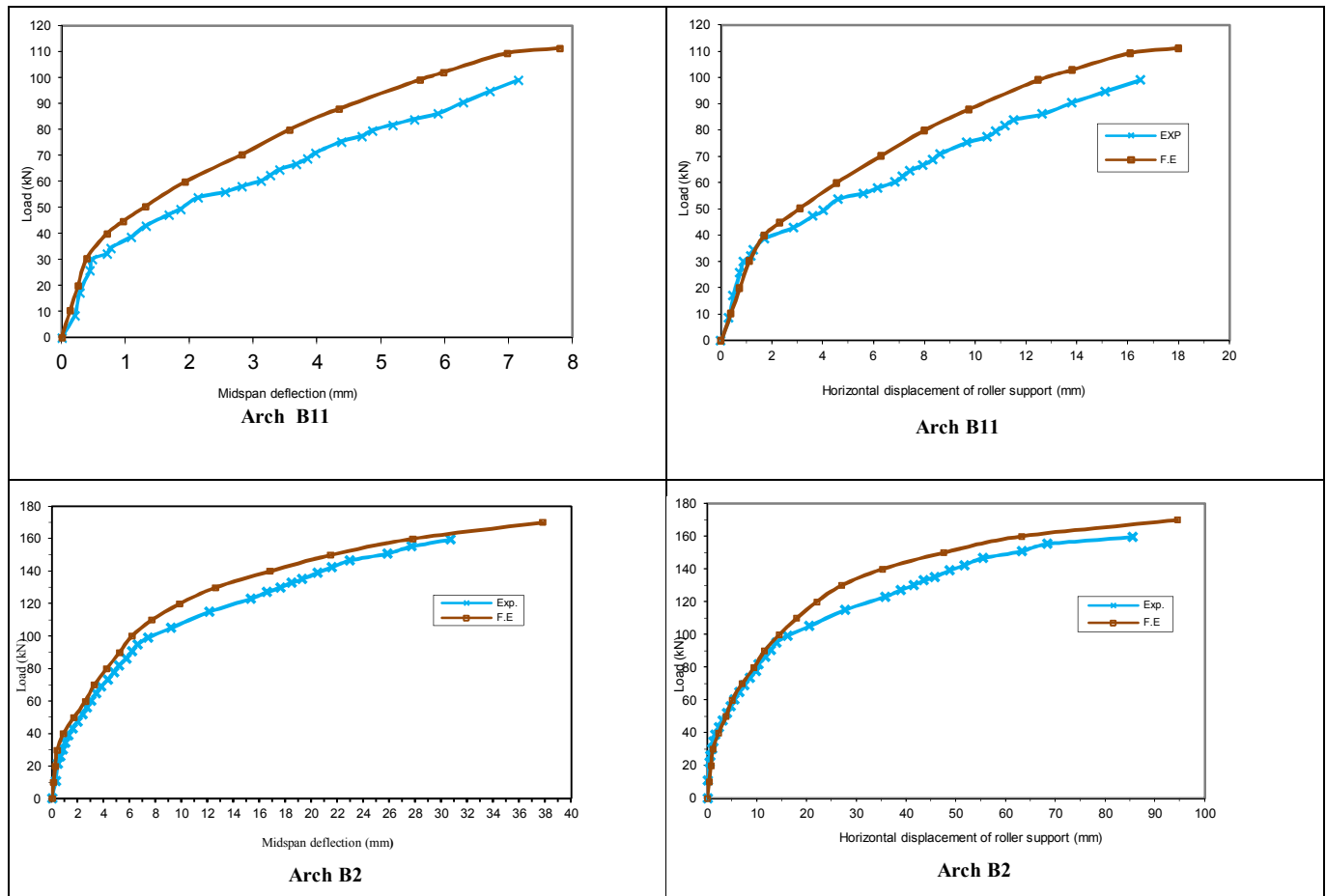
All tested arches (B2 to B12) have been analyzed by using ANSYS computer program to determine the validity of this numerical method for the analysis of RC arches with web opening strengthened externally with CFRP laminates or internally with steel reinforcement. The results obtained from finite element analysis gave good agreement when compared with experimental results which include, cracking load, ultimate load and midspan deflection at service load as explained in Table 4 .

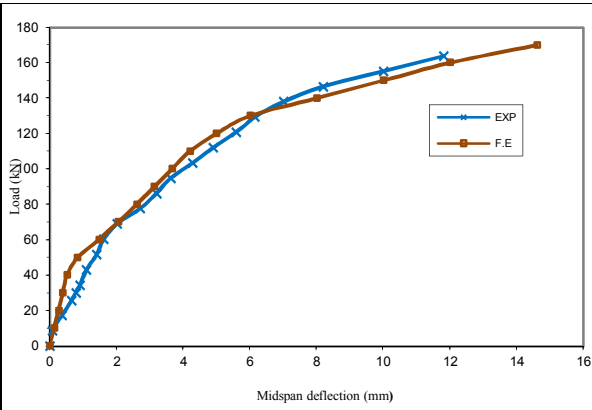
Table 4: Theoretical and Experimental Cracking and Ultimate Loads Comparison

Arch Symbol	Cracking Load (kN)		$\frac{P_{cr}^{theo}}{P_{cr}^{exp}}$	Ultimate Load (kN)		$\frac{P_u^{theo}}{P_u^{exp}}$	Midspan Deflection at Service Load ⁺ , (kN)		$\frac{\delta_{theo}}{\delta_{exp}}$
	P_{cr}^{exp}	P_{cr}^{theo}		P_u^{exp}	P_u^{theo}		δ_{exp}	δ_{theo}	
B11	43.1	36.8	0.85	99.1	111.3	1.12	4.0	2.8	0.68
B2	38.8	35.0	0.90	159.5	170	1.06	8.6	6.3	0.73
B12	60.3	40.0	0.66	163.8	170	1.04	5.2	4.5	0.86
B3(90)	32.3	32.5	1.006	66.8	70.4	1.05	2.5	2.2	0.88
B8(90-S)	25.8	25.0	0.97	142.2	142.5	1.002	10.5	6.0	0.57
B4(90-CF)	34.5	30.0	0.87	133.6	139.5	1.04	7.0	4.8	0.68
B5(45)	25.8	22.5	0.87	64.6	63.75	0.98	2.2	1.8	0.82
B10(45-S)	43.1	37.5	0.87	129.3	139.3	1.08	5.0	5.3	1.06
B6(45-CF)	38.8	39.2	1.01	120.7	123.2	1.02	4.9	4.7	0.96
B7(15)	32.3	32.3	1.00	92.7	102.0	1.10	3.15	3.3	1.05
B9(15-CF)	34.5	37.0	1.07	146.5	150	1.02	6.7	5.4	0.81

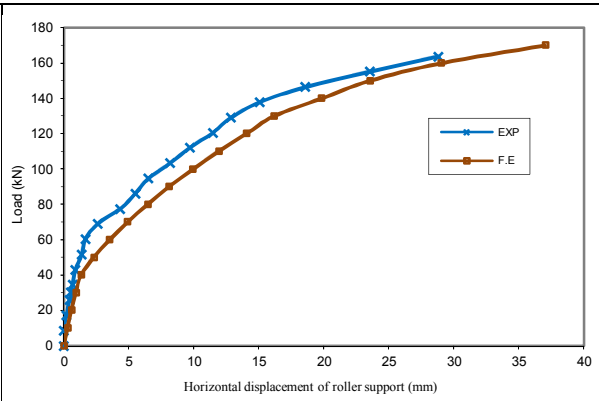
+Service load = $0.70 \cdot P_{u,exp}$

Figure 17 show a comparison between the load-midspan deflection curves and the load-horizontal displacement of roller support curves by the experimental and the numerical results. The variation of mid-span deflection and horizontal displacement of roller support with the applied step-loads for all arches (B2 to B12) are recorded through all these curves. The finite element load-deflection curve for most beams showing a stiffer response rather than the experimental results. Microcracks produced by drying shrinkage and handling are presenting in the concrete; these would reduce the stiffness of the actual beam, while the F.E. does not include the effect of microcracks. The F.E. analyses assume that concrete is a homogenous material but, the true it is a heterogeneous material. Also, a perfect bond between the concrete and steel and also, between concrete and CFRP laminates is assumed in the F.E. analysis. However, the assumption would not be true in the actual beam. The comparison shows the validity of the FEM results and the program used in application (ANSYS) by showing a reasonable agreement with the experimental results discussed previously.

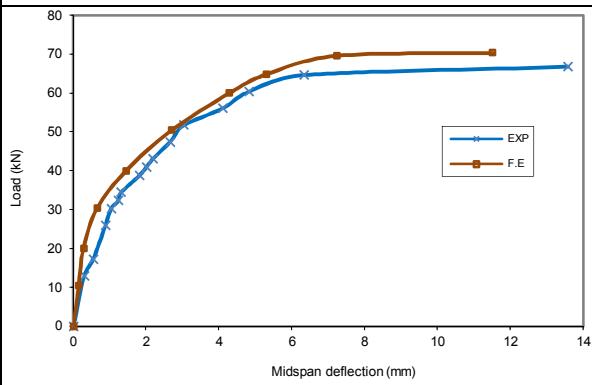




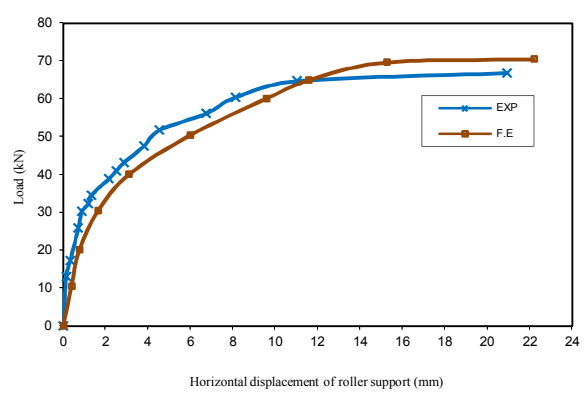
Arch B12



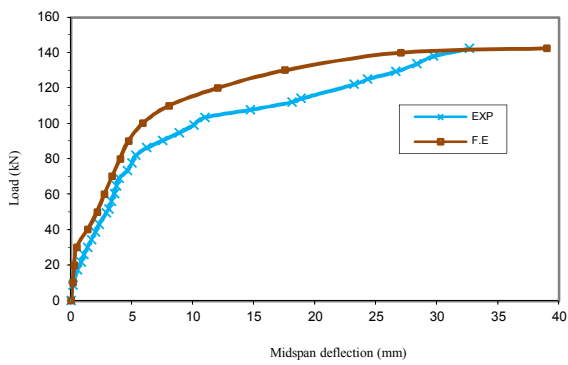
Arch B12



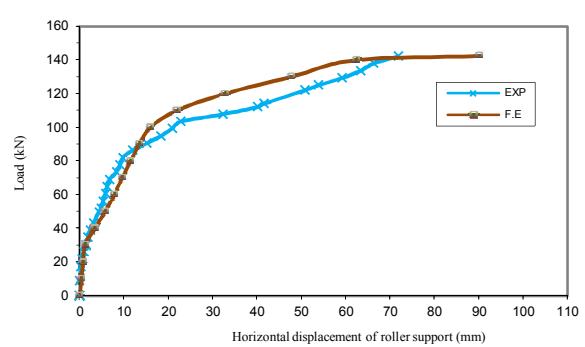
Arch B3(90)



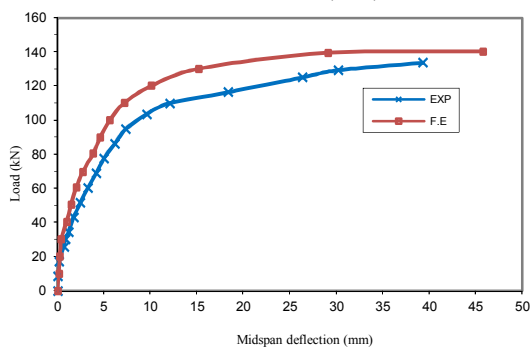
Arch B3(90)



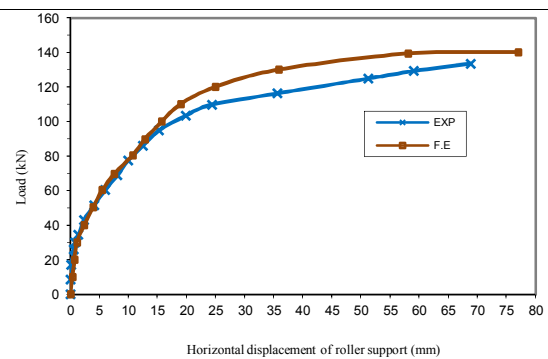
Arch B8(90-S)



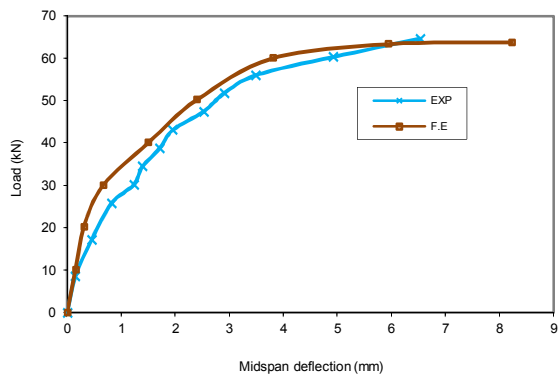
Arch B8(90-S)



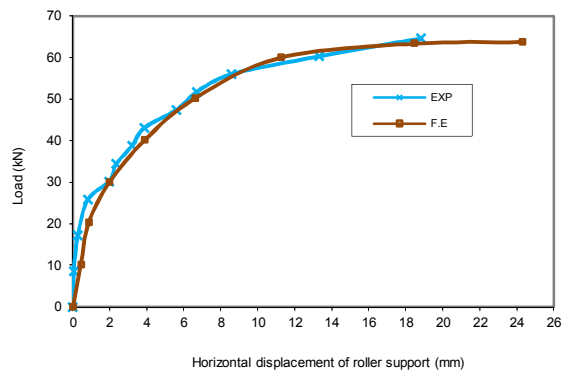
Arch B4(90-CF)



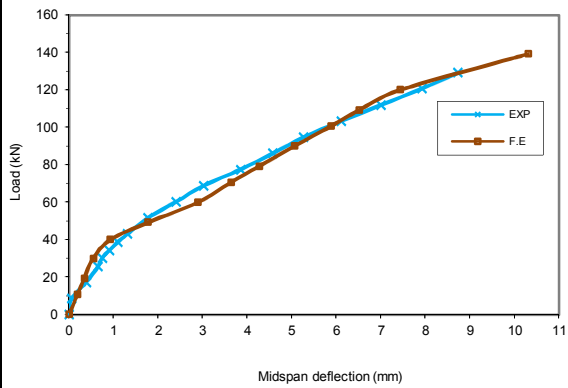
Arch B4(90-CF)



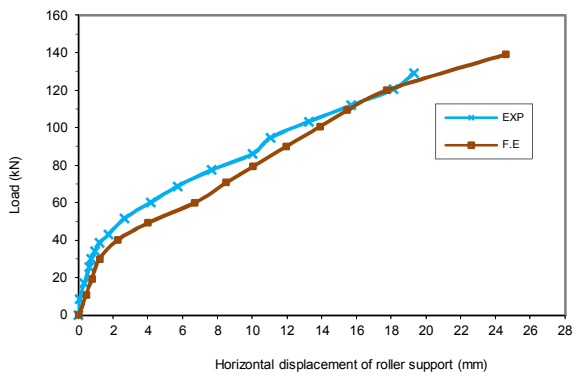
Arch B5(45)



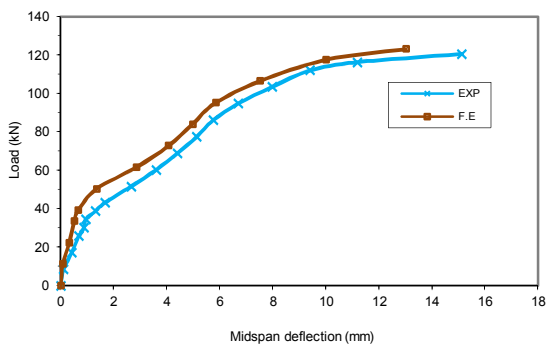
Arch B5(45)



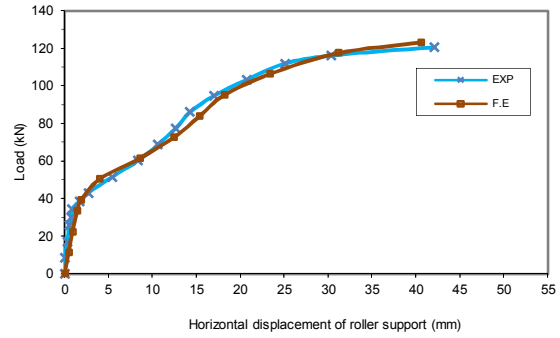
Arch B10(45-S)



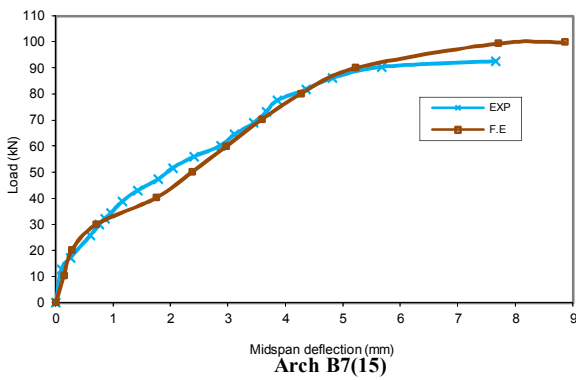
Arch B10(45-S)



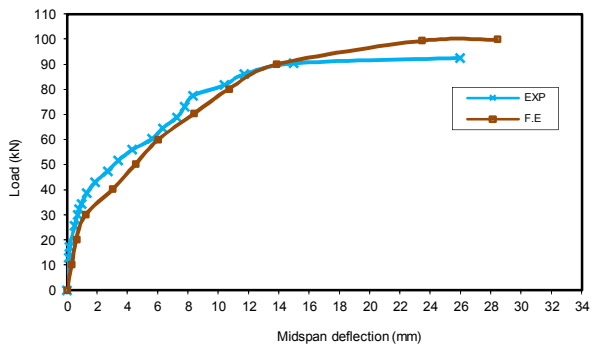
Arch B6(45-CF)



Arch B6(45-CF)



Arch B7(15)



Arch B7(15)

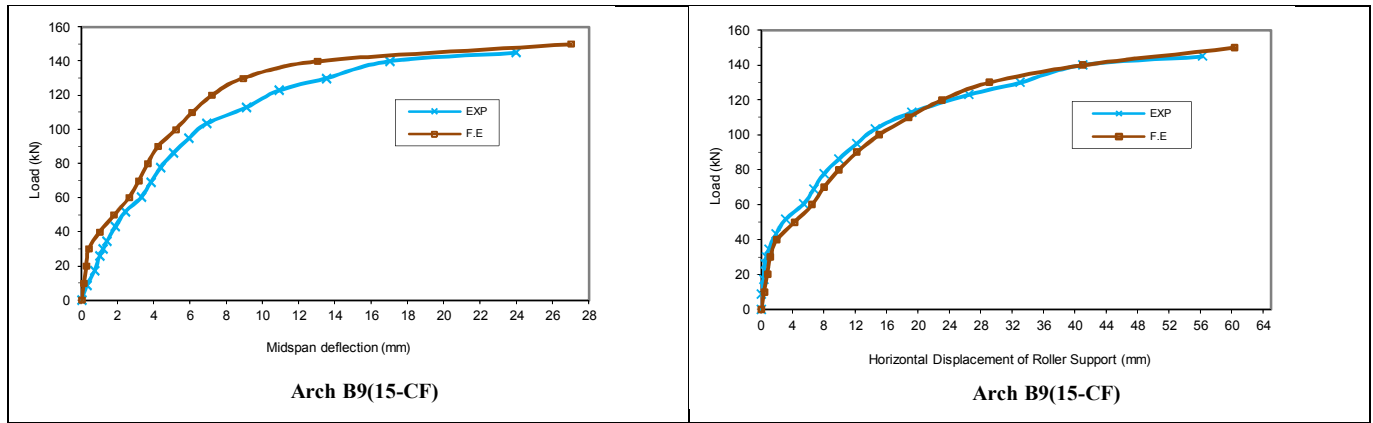


Figure 17 :Experimental and theoretical load-deflection curves for tested arches

Conclusion

- 1- In the absence of internal confining stirrups or external CFRP straps to resist curvature forces induced between reinforcing bars and concrete cover, a sudden splitting failure will occur without any warning in addition to decreasing in load carrying capacity by about 38%.
- 2- The use of CFRP laminates as external confinement instead of internal stirrups at the middle sector to resist curvature forces induced between reinforcing bars and concrete cover, gave approximately the same general response, but the ductility ratio was lesser.
- 3- The external strengthening by CFRP laminates enhanced the general behavior of strengthened arches in terms of (ductility ratio, mode of failure , crack pattern and ultimate load) in comparison with unstrengthened arch.
- 4- The increase in load carrying capacity for arch containing an opening at zone of excessive compressive force (near the support) was 39% and 43% more than for zones (pure bending and combined of bending, shear force and axial compressive force), respectively.
- 5- The design method proposed herein for internal strengthening of opening at constant moment (pure bending) gave good result, where the mode of failure changed from failure of opening mode to flexural failure mode. The reduction in ultimate load of strengthened arch was about 11% as compared with that of solid control arch. Also, there was an increase in the ultimate load by about 113% when compared with unstrengthened arch.
- 6- The method of design suggested by Mansure (1998) for straight beam, used herein to internally strengthening of opening at region of combined bending, shear and axial compressive forces, gave ultimate load of about 81% of solid control arch, and the mode of failure does not change (still within opening).
- 7- The design method proposed herein for external strengthening with CFRP laminates of opening at pure bending region and combined of shear force, moment and axial compression

force region, gave ultimate load of about 83% and 75%, respectively of solid control arch, and the mode of failure does not change (still within opening).

- 8- The design method proposed herein for external strengthening with CFRP laminates of opening at excessive axial force (near to support), gave good result and the mode of failure changed from failure of opening mode to flexural mode.
- 9- For arch with unstrengthened opening near the supports, the minimum distance from support to the edge of the opening(one-half of beam depth), which had been given by Tan and Mansure (1996) for straight beam, was not valid for arches.
- 10- The general response of externally strengthened arches by CFRP laminates was approximately in agreement with arches of internally strengthened by steel stirrups in terms of (load-deflection curves, crack pattern. Cracking and ultimate loads with average difference 5.83% and 3.92%, respectively).
- 11- The general behavior of the finite element models which were analyzed by (ANSYS version 11.0)represented by load-midspan deflection and load-horizontal displacement of roller support plots showed reasonable agreement with test data plots for tested arches.
- 12- The comparison between the F.E. analysis and the experimental results that asserted the validity of the numerical analysis by (ANSYS version 11.0) shows maximum deviation in ultimate load of about 12%.

References

- (1) Mansur, M.A., (2006) " Design of Reinforced Concrete Beams with Web Openings " Proceeding of the 6th Asia-Pacific Structural Engoneering and Construction Conference (APSEC 2006), 5-6 September, Kuala Lumber, Malaysia.
- (2) Mansur, M.A., and Hasnat A. (1979) "Concrete Beams with Small Openings under Torsion" Journal of the Structural Division, ASCE, Vol. 105, No. ST11, November, pp. 2433-2447.
- (3) Somes, N.F. and Corley, W.G., (1974), "Circular openings in webs of continuous beams", SP-42, American Concrete Institute, Detroit, MI, pp. 359- 398.
- (4) Mansur, M.A., (1998) "Effect of Openings on the Behavior and Strength of R/C Beams in Shear" Cement and Concrete Composites, 20, pp. 477-486.
- (5) Ali, H.,A.,(2006),"Flexural and Shear Behavior of Hybrid I-Beams With High Strength Concrete and Steel Fibers" Ph.D. Thesis, University of Al-Mustansiriya.
- (6) Bashar, A.,H.,(2013),"Behavior of RC Curved Beams with Openings and Strengthened by CFRP laminates" Ph.D. Thesis, University of Basrah.

- (7) Tan K.H., and Mansur M.A., (1996) "Design Procedure for Reinforced Concrete Beams with Large Web Openings" ACI Structural Journal, Vol. 93, No. 3, July-August.
- (8) ACI Committee 318, (2011) "Building Code Requirements for Structural Concrete (ACI318M.11) and Commentary", American Concrete Institute, Farmington Hills, Michigan, USA, 473 pp.
- (9) ACI Committee 440, (2002) "Guide for the design and Construction of externally Bonded FRP Systems for Strengthening of Concrete Structures", American Concrete institute, Michigan, USA.
- (10) Sika CarboDur FRP Composites Constrection for Repair & Strengthening of Structures . MARCH 2003 .
- (11) "ANSYS Manual", Version (11.0), USA, 2007.